Talanta 115 (2013) 500–505

Contents lists available at SciVerse ScienceDirect

Talanta

journal homepage: www.elsevier.com/locate/talanta

Electrodeposited apatite coating for solid-phase microextraction and sensitive indirect voltammetric determination of fluoride ions

Yuehong Mao, Yufei Chen, Lin Chu, Xiaoli Zhang*

School of Chemistry and Chemical Engineering, Shandong University, Jinan 250100, China

ARTICLE INFO

Article history:
Received 8 March 2013
Received in revised form
6 June 2013
Accepted 10 June 2013
Available online 15 June 2013

Keywords:
Electrodeposition
Apatite coating
Solid-phase microextraction
Fluoride ions
Indirect determination

ABSTRACT

Electrodeposition was used to prepare a new solid phase microextraction (SPME) coatings. Two apatite SPME coatings, dicalcium phosphate dihydrate (DCPD or brushite) and hydroxyapatite (HAP) were validly and homogeneously one-step electrodeposited on glassy carbon electrode (GCE) under different conditions. The coatings were characterized by XRD, FTIR, SEM, CV and EIS. The apatite SPME coatings showed excellent and selective adsorbability to fluoride ions. A novel indirect voltammetric strategy for sensitive detection of fluoride was proposed using $K_3Fe(CN)_6$ as indicating probe. The detection principle of fluoride ions was based on the increment of steric hindrance after fluoride adsorption, which resulting in the decrease of the amperometric signal to $Fe(CN)_6^{3-}$. The liner ranges were 0.5–20.0 μmol/L for *n*-DCPD/GCE with the limit of detection of 0.14 μmol/L and 0.1–50.0 μmol/L for *n*-HAP/GCE with the limit of detection of 0.069 μmol/L, respectively. The developed method was applied to the analysis of water samples (lake, spring and tap water) and the recovery values were found to be in the range of 90–106%.

1. Introduction

Solid-phase microextraction (SPME), developed by Pawliszyn and co-workers [1], is a simple, rapid and solvent-free preparation technique since it has been introduced in the early 1990s. Hence the SPME has been well developed [2]. The key of the technique is the extraction fiber [3]. In this regard, different coating techniques have been introduced including pasting with adhesives, electrochemical polymerization or deposition, direct pasting, chemical corrosion, and the sol–gel technique [4]. Among all the techniques, electrodeposition offers important advantages, such as a rigid control of the film thickness formed, uniformity and fast deposition rate.

Fluoride is an essential constituent for animals including humans [5]. However, the total amount ingested or its concentration in drinking water must be within certain limits [6]. It is very important for us to detect fluoride ions. At present, the most popular technique for fluoride ions detection is fluoride ion selective electrode (ISE) [7], fluorescence analysis [8], gas chromatography and liquid chromatography [9]. There are some limitations in these methods. The response of ISE needs long time for signal obtaining because it takes much time for equilibrium establishment. Fluorescence analysis is often associated with organic chemicals which are environment-unfriendly and chromatography is expensive. Therefore, a reliable, simple, fast, sensitive, and cost-effective method for fluoride ions detection is asked to propose.

In recent years, removal of fluoride from aqueous solution by adsorption is a simple and attractive strategy due to its high efficiency and easy handling [10]. Various apatite materials were found to be a suitable sorbent for fluoride because of their low costing, availability and high adsorption efficiency as previously reported in the literature [11]. The apatite materials can be fabricated by employing many chemical-based processing routes for example solid-state reaction, sol–gel technique, biosynthesis route, wet chemical route, chemical precipitation, hydrothermal reaction, microwave heating, microemulsions and recently electrodeposition method [12–15]. One-step electrodeposition of apatite [16] has attracted significant interest for sensing applications owing to their excellent stability and good biocompatibility [17].

Herein, we attempted to use apatite coatings prepared by electrodeposition as SPME fibers for fluoride extraction. The apatite SPME coatings (DCPD and HAP) were directly electrodeposited onto GCE from the electrolyte solution containing $Ca(NO_3)_2{\cdot}4H_2O$–$NH_4H_2PO_4$ via a constant potential of −1.0 V (vs. SCE) for 500 s. The resulting SPME fibers displayed selective and particular adsorbability to the fluoride ions. A novel sensitive indirect voltammetric determination method of fluoride ions was proposed using $K_3Fe(CN)_6$ as indicating probe. The introduction of indicating probe solved the problem that the direct oxidation–reduction of fluoride ions is difficult. The experiment mode was based on the change of current signal before and after fluoride extraction, and a new method for detecting fluoride ions was

* Corresponding author. Tel.: +8653188361318; fax: +8653188564464.
E-mail address: zhangxl@sdu.edu.cn (X. Zhang).

0039-9140/$ - see front matter © 2013 Elsevier B.V. All rights reserved.
http://dx.doi.org/10.1016/j.talanta.2013.06.013

developed. The apatite was characterized by XRD, FTIR, SEM, CV and EIS. Analytical performances of the proposed SPME approach were tested. Finally, three real water samples were employed to this method with satisfactory results.

2. Experimental

2.1. Apparatus

A CHI 800 electrochemical analyzer (Shanghai Chenhua Instrument Company, China) was used to perform electrode characterizations and voltammetric measurements. A conventional three-electrode system including a glassy carbon electrode (GCE, 3 mm diameter) or modified GCE as working electrode, a platinum wire as counter electrode and a saturated calomel electrode (SCE) as reference electrode was used in this work.

2.2. Reagents

Sodium fluoride was obtained from Shanghai Xinhua Chemical Regent Corporations Ltd. (China). Calcium nitrate and ammonium dihydrogen phosphate was obtained from China National Pharmaceutical Group Corporations Ltd. (China). $K_3Fe(CN)_6$ was purchased from Sinopharm Chemical Reagent Beijing Corporations Ltd. (China). All the reagents were of analytical reagent grade and used as received. Electrolytic solutions were prepared using ultrapure water (Ulupure, Chengdu, China, 18.2 MΩ resistivity) and deaerated with nitrogen. All electrochemical measurements were conducted in deaerated solutions. The experiments were performed at room temperature, 298 K.

2.3. Preparation of the apatite SPME coating

The GCE was polished repeatedly using alumina powder (0.50, 0.30 and 0.05 μm) and thoroughly cleaned. The GCE was immersed into the electrolyte containing 0.23 mol/L $Ca(NO_3)_2 \cdot 4H_2O$ and 0.14 mol/L $NH_4H_2PO_4$ (deoxygenization for 1 min in nitrogen flow, pH 3.0). The electrodeposition was conducted at −1.0 V for 500 s with the magnetic stirring controlled at 60 rpm to keep the concentration uniform. The resulting electrode, *n*-DCPD SPME coating modified GCE, was activated by several successive cyclic voltammetry from −0.2 to 1.4 V with a scan rate of 50 mV/s in phosphate buffer (pH 7.0) until a steady voltammogram was obtained. To obtain the n-HAP SPME coating, steps were all the same to the former except that the pH value of the electrolyte was adjusted to 7.0 with ammonia before electrodeposition. They were stored in a refrigerator (4 °C) when not used.

2.4. Extraction and detection for fluoride ions

First, the apatite SPME coating modified electrode (*n*-DCPD/GCE or *n*-HAP/GCE) was immersed into the solution of fluoride ions for extraction (through an accumulation of 10 min on open circuit). After being taken out, the *n*-FD/GCE or *n*-FHA/GCE (after *n*-DCPD/GCE or *n*-HAP/GCE extracting fluoride ions) was obtained. Subsequently, the electrode with fluoride ions (*n*-FD/GCE or *n*-FHA/GCE) was performed the stripping voltammetric detection in another supporting electrolyte of KCl containing $K_3Fe(CN)_6$ as indicator. The voltammogram was recorded from 0 to 0.5 V and the peak height was measured as a signal (I). The corresponding voltammogram of blank modified electrode (before extraction) was recorded and the peak height was marked as I_0. The quantification of fluoride was achieved based on the change of current signal ΔI ($\Delta I = I_0 - I$) with the fluoride ions concentration.

3. Results and discussion

3.1. X-ray diffraction, fourier transform infrared spectrum and scanning electron microscopy

The prepared apatite coating was characterized by X-ray diffraction (XRD, Rigaku D/MAX-rA). The XRD data were collected from 10° to 70° using Cu $K\alpha$ radiation at 40 kV and 40 mA. The crystalline phases were determined from a comparison of the XRD patterns with the JCPDS powder diffraction file. Fig. 1 represents XRD patterns of the DCPD, FD, HAP, and FHA. For DCPD, the most-prominent peak, which was situated at an angle of $2\theta = 11.7°$, corresponded to the DCPD (0 2 0) peak. The XRD results also showed typical crystallized peaks of DCPD at $2\theta = 20.9°$ and $2\theta = 29.3°$. All the well-defined diffraction peaks in graph were identical to the pattern of JCPDS card 09–0077, confirming the formation of DCPD on the surface of GCE. After extracting fluoride 10 min on open circuit, *n*-FD/GCE was obtained. For FD, there were some significant changes in the scalar and location of diffraction peaks, for instance, crystal faces (0 2 1), (0 4 1) of the brushite peaks were not found in spectrum. Only amorphous particles were possible to see. The results represented that fluoride ion had been inserted into DCPD and damaged its structure. As presented in XRD patterns of HAP and FHA, the most intensive peaks were the (3 0 0), (2 1 1), and (0 0 2) peaks. In addition, there were weaker peaks, (3 1 0), (2 2 2), (2 1 3) and (3 2 3) according to the PDF data base. For the FHA, almost all the crystal diffraction remained by comparison with the HAP, indicated that there were no significant changes in the crystal shape. However, the diffraction intensities of three peaks around $2\theta = 32°$ were decreased obviously after the fluoride ions extraction. Many literatures [10,11,18] reported that hydroxyapatite had the sorption behavior for fluoride ions. This behavior could be attributed to the presence of OH^- that might compete with F^- for the sorption sites in the sorbent material [18,19], the possible reaction process of F^- at the *n*-HAP/GCE was as followed in our work:

$$Ca_{10}(PO_4)_6(OH)_2 + 2xF^- + 2xH^+ \rightarrow Ca_{10}(PO_4)_6F_{2x}(OH)_{2-2x} + 2xH_2O$$

As for the decrease of the diffraction intensity, the reason might be that the excess fluoride ions were full of the nano-porous

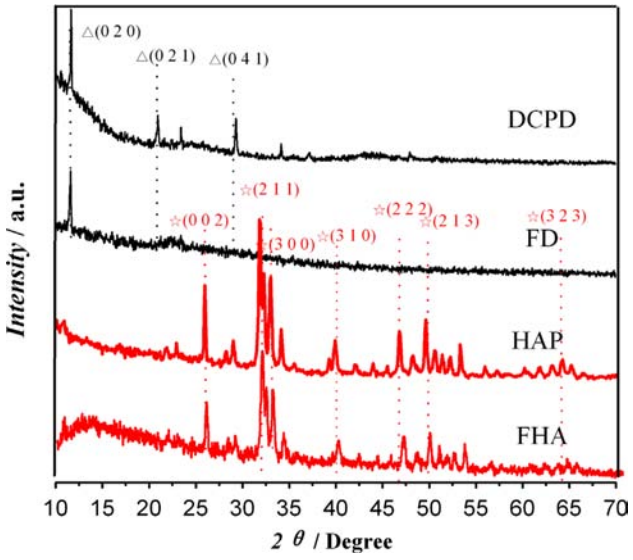

Fig. 1. XRD of *n*-DCPD, *n*-HAP, *n*-FD and *n*-FHA. Symbol △ was for *n*-DCPD or *n*-FD. Symbol ☆ was for *n*-HAP or *n*-FHA. Two apatite SPME coatings were obtained by electrodepositon at −1.0 V for 500 s. The initial concentration of fluoride ions for extraction was 40.0 μmol/L.

apatite SPME coating, leading to the lattice damage of some FHA molecules.

Fourier transform infrared spectra (FTIR) were taken on Bruker Germany α-ALPHA-T spectrophotometer. Sample of the apatite coating was mixed with KBr powders under the infrared lamp bake, homogenized and converted into pellets under a pressure of 25 MPa. The spectra (% transmittance with wave number) were taken thereafter.

Considering that the evidence of the presence of FHA was still incomplete by the XRD data, the FTIR spectra of *n*-HAP SPME coating before and after fluoride ions extraction were given in Fig. 2. The FTIR spectra of HAP matched well with the spectra reported by others [20,21]. The peak bonds at about 3572 and 634 cm^{-1} which were clearly visible in the FTIR spectra of the two samples belong to the stretching vibrations of hydroxyl. The peaks at about 566, 603 cm^{-1} must be due to the bending vibration and 962, 1034 and 1093 cm^{-1} to the stretching vibration of PO_4^{3-} group. For the *n*-FHA, the vibration between fluorine and phosphorus at about 830 cm^{-1} showed a weak singlet. This certificated that the fluoride ions were inserted into the *n*-HAP SPME coating. In addition, the bonds intensity at 3572 and 634 cm^{-1} of the stretching vibrations of hydroxyl in FHA has decreased. It could be explained by fluoride adsorption/exchange: Fluorine replaced the position of hydroxyl in the nano-structure. The reduction of hydroxyl in the HAP coating leads to the bond energy decreased immediately, indirectly reflecting that the *n*-FHA was generated.

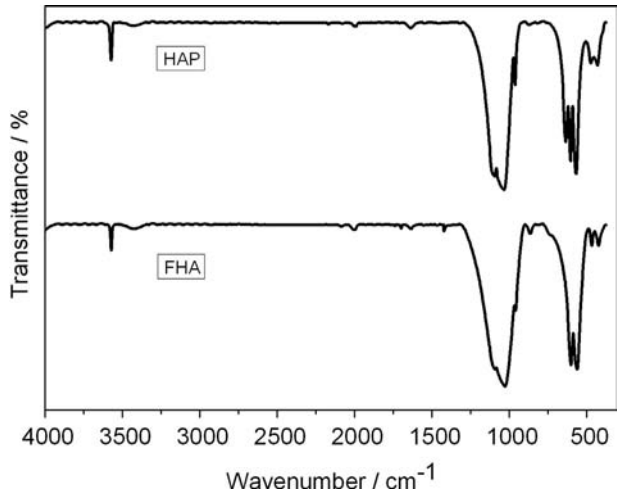

Fig. 2. FTIR spectrum of *n*-HAP and *n*-FHA. The *n*-HAP and *n*-FHA were prepared in the same conditions as in Fig. 1.

The surface topography of the *n*-DCPD SPME coatings before and after fluoride extraction was observed with a scanning electron microscope (SEM, JSM-6700F, Japan), shown in Fig. 3. It could be seen the channel structure of the DCPD crystals appeared on the surface of GCE (Fig. 3a), which possess nano-porous structure. SEM images of *n*-DCPD/GCE after fluoride ions extraction were shown in Fig. 3b–f. Compared with that in Fig. 3a, the mesh in DCPD surface shrinked and even disappeared, indicating that the fluoride ions had inserted into and damaged the nano-structure of the *n*-DCPD coating.

Two ways were used to make fluoride ions extraction: one was open circuit accumulation under stirring, the other was simple immersion. The results indicated that former (Fig. 3b) could accelerate the diffusion of fluoride ions from solution to electrode surface, leading to a more effective enrichment compared with simple immersion (Fig. 3c). Besides, the experiments from different immersion time also manifested that the 24-h immersion gave fluoride ions full time to react with the *n*-DCPD, which resulting in the holes in *n*-DCPD structure disappeared thoroughly (Fig. 3d).

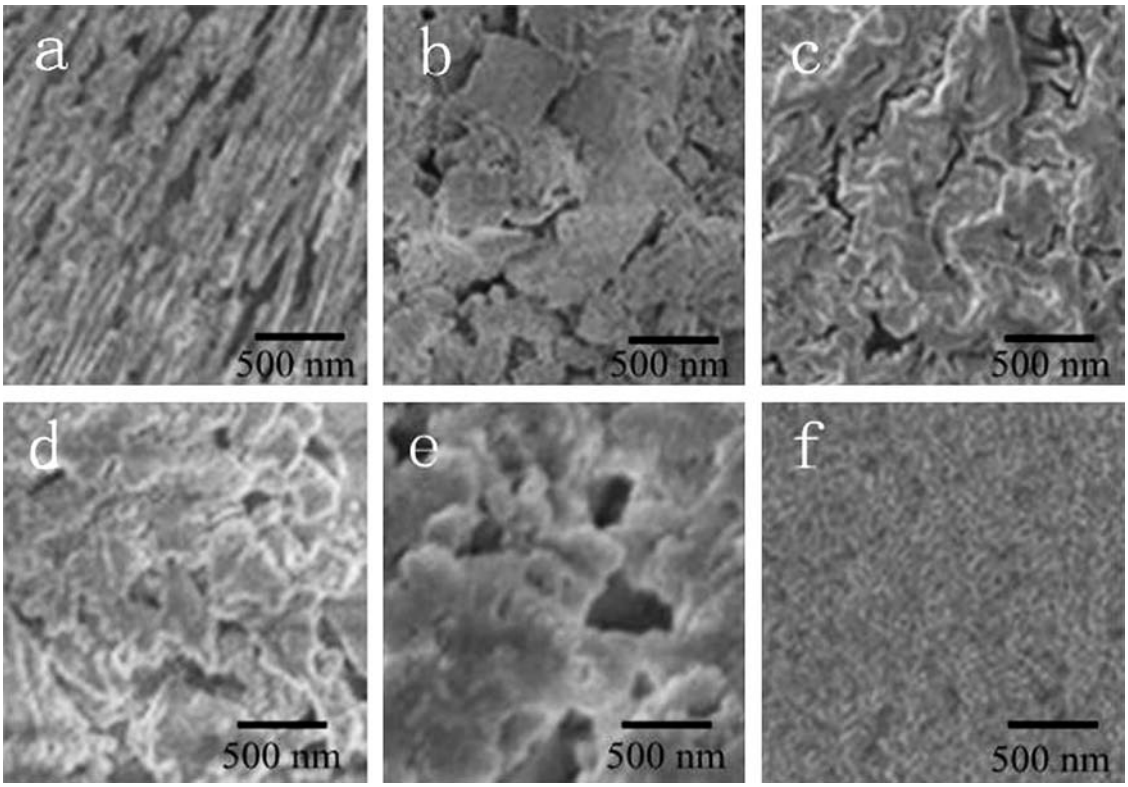

Fig. 3. SEM pictures of (a) *n*-DCPD/GCE and ((b)–(f)) *n*-FD/GCE. The *n*-DCPD/GCE was prepared in the same condition as in Fig. 1. The experimental conditions (extraction way, extraction time and fluoride ions concentration) of ((b)–(f)) were as follows: (b) simple immersion, 10 min, 10.0 μmol/L NaF, (c) simple immersion, 24 h, 10.0 μmol/L NaF, (d) open circuit enrichment, 10 min, 10.0 μmol/L NaF, (e) open circuit enrichment, 10 min, 100.0 μmol/L NaF, (f) open circuit enrichment, 10 min, 1000.0 μmol/L NaF.

Fig. 3b, e and f were the images about different fluoride ions concentrations. In Fig. 3b, nano-porous structure could be easily observed. When the concentration of fluoride ions increased (Fig. 3e), the mesh was mostly covered by fluoride material and the holes could hardly be observed in Fig. 3f. It looked like a uniform layer of film on the electrode. Obviously, the higher concentration allowed the faster free entry of fluoride ions into the inner layers under the same enrichment time.

3.2. Cyclic voltammetry and electrochemical impedance spectroscopy

The electrochemical characterizations were performed by cyclic voltammetry (CV) and electrochemical impedance spectroscopy (EIS). As shown in Fig. 4, at GCE, a couple of well defined redox peaks with peak-to-peak separation (ΔEp) of 70 mV were observed. The voltammogram of *n*-DCPD/GCE displayed that ΔEp was 100 mV. The current of the anodic and cathodic peaks were 42% and 48%, respectively, lower than that observed at the GCE, indicating that DCPD coating hindered electron conduction. For *n*-HAP/GCE, ΔEp was 80 mV. The current of 74% anodic and 70% cathodic peaks were remained. The *n*-HAP/GCE exhibited more reversible than *n*-DCPD/GCE. When *n*-DCPD/GCE (or *n*-HAP/GCE) was immersed in 40.0 μmol/L fluoride ions solution for fluoride extraction, the *n*-FD/GCE (or *n*-FHA/GCE) was obtained. The resulting electrodes also exhibited a couple of redox peaks, but with a lower current signal response than *n*-DCPD/GCE (or *n*-HAP/GCE). These decrease of the amperometric signals to $K_3Fe(CN)_6$ had two main reasons. First, the fluoride ions inserted into the nanostructure, leading to the increment of steric hindrance. Next, formed FD (or FHA) with poor electrical conductivity could hamper the electron transport from the electrode surface to the electrolyte.

EIS was performed over a frequency range from 10 mHz to 100 kHz with perturbation amplitude of 0.01 V. The Nyquist diagrams formed by semi-circle and straight line curves were shown in Fig. 5. The semi-circle of each graph followed the order: FHA > FD > DCPD > HAP > GCE. Compared with the bare GCE (insert), the semi-circle of *n*-HAP/GCE or *n*-DCPD/GCE increased. This indicated that the electron transfer resistance at the electrode/electrolyte interface increased after the apatite SPME coating electrodeposition. Furthermore, the semi-circle of *n*-HAP/GCE was smaller than that of *n*-DCPD/GCE. This certificated that HAP had a better electric conductivity than DCPD under this circumstance. Besides, the impedance value of the apatite SPME coating

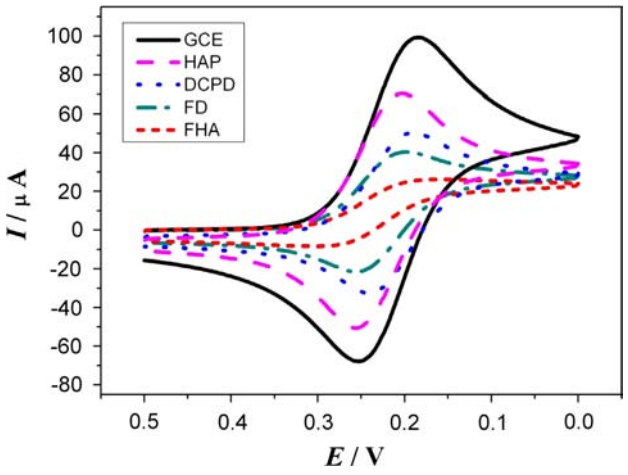

Fig. 4. CVs of bare GCE, *n*-DCPD/GCE, *n*-HAP/GCE, *n*-FD/GCE and *n*-FHA/GCE in 0.01 mol/L $K_3Fe(CN)_6$ solution using 0.50 mol/L KCl. The scan rate was 50 mV/s. Four modified electrodes were prepared in the same conditions as in Fig. 1.

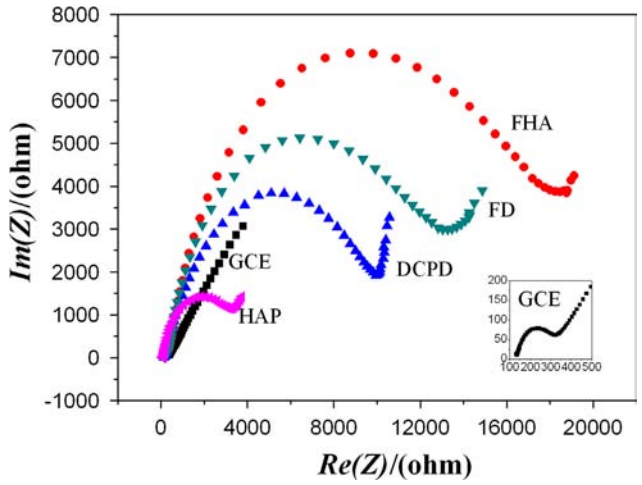

Fig. 5. EIS spectrum of bare GCE, *n*-DCPD/GCE, *n*-HAP/GCE, *n*-FD/GCE and *n*-FHA/GCE in 0.50 mol/L KCl solution containing 5.0 mmol/L $K_3Fe(CN)_6/K_4Fe(CN)_6$.

after fluoride extraction was even larger than before. After extracting fluoride ions, leading to the coating being more insulating. In presence of $K_3Fe(CN)_6$ as external redox probe, it was found that HAP had a better fluoride absorption ability than DCPD, as also supported by the CV data.

3.3. Optimization of SPME preparation and fluoride detection conditions

To improve the performance of the apatite SPME coating for sensitive detecting F^-, the effect of preparation conditions (electrodeposition potential and time), extraction time and concentration of indicating probe on the current signal (ΔI) were investi&hyphen-qj;gated in detail.

The electrodeposition conditions could alter the morphology of the deposited nano-apatite SPME coating and played an important role in the process of fluoride extraction. Therefore, based on the current signal value (ΔI), electrodeposition conditions were optimized. In this part, 40.0 μmol/L fluoride ions were chosen as the initial concentration. As seen from Fig. 6A, with the increase of electrodeposition potential from −0.2 to −1.0 V, the ΔI enhanced gradually. When the potential was −1.0 V, the largest ΔI was obtained. Fig. 6B depicted the influence of electrodeposition time on the ΔI. With the electrodeposition time increasing, the ΔI enhanced until the time reached 500 s. When the time exceeded 500 s, the ΔI decreased gradually, which suggested that the modified coating was thick and it was not beneficial for fluoride ions sensing. So, electrodeposition potential of −1.0 V and electrodeposition time of 500 s was chosen.

The effect of extraction time on ΔI was also studied (shown in Fig. 6C). For both *n*-DCPD and *n*-HAP, it was clear that the ΔI increased remarkably within the first 8 min and then enhanced slowly. Further increase of the extraction time did not increase the ΔI so much, owing to the amount of fluoride ions at the apatite surface become saturated, leading to ΔI was nearly constant. This phenomenon was explained by the interaction between F^- and the nano-apatite SPME coating. A further control experiment was made. When bare GCE was immersed into the solution containing fluoride ions for 10 min extraction (preconcentration), no obvious increase on the ΔI could be obtained. This demonstrated that the bare GCE had poor absorbability towards F^-.

The concentration of $K_3Fe(CN)_6$ used as indicating probe could inhibited the sensitivity of detection for fluoride ions greatly. Obviously, when the concentration of probe, $K_3Fe(CN)_6$ was too high (larger than 0.01 mol/L), trance amount of fluoride ions only

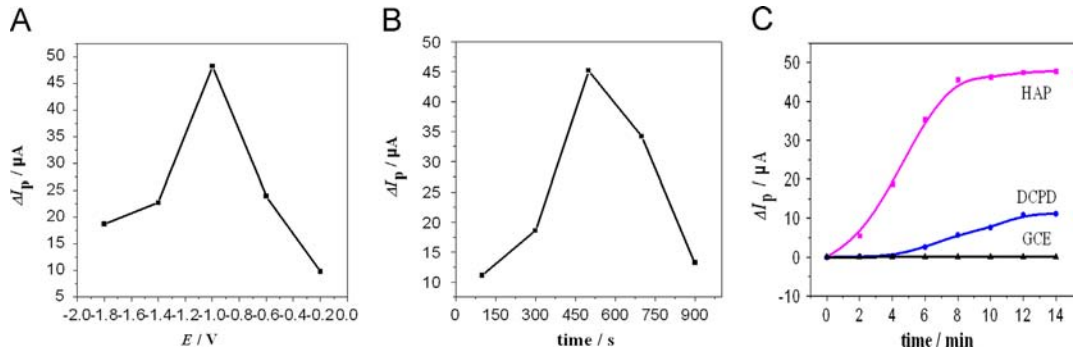

Fig. 6. Effect of electrodeposition potential (A), electrodeposition time (B) and extraction time (C) on the current signal. (A) *n*-DCPD/GCE, (B) *n*-DCPD/GCE, (C) GCE, *n*-DCPD/GCE and *n*-HAP/GCE. Experimental conditions were the same as in Fig. 1, except for electrodeposition potential, electrodeposition time or extraction time.

generated an inconspicuous current signal, which was difficult to test. However, when the concentration of probe was smaller than 0.01 mol/L, the base current signal (I_0) was so little that the detectability was restrained. Considering for these, 0.01 mol/L was chosen as the concentration of $K_3Fe(CN)_6$.

3.4. Calibration curve, reproducibility and interference

The analytical performance and characteristics of the proposed SPME approach for detection of fluoride ions were tested. In these systems of *n*-DCPD-F^- or *n*-HAP-F^-, the fluoride ions concentration had a linear relationship with the change current signal (ΔI) of indicating probe. The regression equation of *n*-DCPD/GCE was ΔI (μA)=0.0554+0.1124 c (μmol/L), with a correlation coefficient of 0.9964 and the liner range 0.5–20.0 μmol/L. The limit of detection was 0.14 μmol/L ($S/N=3$).

For n-HAP/GCE, with the increase of fluoride concentration, the change of current signal (ΔI) increased. As Fig. 7 shown, the ΔI had two linear relationships ranged from 0.1 to 2.0 μmol/L and 2.0 to 50.0 μmol/L. The detect limit was found to be as low as 0.069 μmol/L. The regression equation were ΔI (μA)=−0.1048 +5.3796 c (μmol/L) ($R^2=0.9978$) and ΔI (μA)=10.880+1.1981 c (μmol/L) ($R^2=0.9918$), respectively. At the same time, it could be seen that the slope at high concentration was smaller than that at low concentration. The possible reason was that the adsorption dynamics of fluoride ions was faster at low concentration than that at high concentration.

The repeatability of apatite SPME coating modified electrodes had also been studied. The relative standard deviation (RSD) of the current response of *n*-HAP/GCE to 5.0 μmol/L fluoride ions was 3.6% for five successive measuremrnts. For ten electrodes modified identically, the RSD was 5.8% (lower than 10%), revealing that this method had good repeatability.

The interference of some foreign species found in water pollutants on the detection of fluoride ions was individually examined within 5.0 μmol/L fluoride ions. For *n*-DCPD/GCE or *n*-HAP/GCE, a thousand-fold excess of Cl^- and a hundred-fold excess of SO_4^{2-}, NO_2^-, Mg^{2+}, Mn^{2+}, Fe^{3+} and a 10-fold excess of Cu^{2+}, Zn^{2+} had little influence on the current signals with deviations below 5%. This modified electrode showed satisfactory anti-interference ability. It was suitable for fluoride ions analytical applications.

3.5. Real sample analysis

Fluoride ions are ubiquitously contaminants in the waters and the overdose of fluoride are serious enough to threaten the public health. Three water samples (lake, spring and tap water, which was from Daming lake, Baotu spring of Jinan city, China, diluted for one hundred times) were chosen to investigate the reliability of the as-prepared *n*-DCPD/GCE or *n*-HAP/GCE. As we can see from Table 1, the concentration of fluoride ions were detected in the three water samples and their concentration can be quantified to 520, 310, 160 and 560, 340, 180 μmol/L. In order to demonstrate the applicability and reliability of the method, the dose of the fluoride ions were also determined by fluoride ion selective electrode (ISE) in the three water samples, with the concentration 550, 360 and 200 μmol/L, respectively. Fairly close results were obtained by the proposed SPME methods and ISE method. To examine the recovery, a known amount of fluoride ions was added to the sample. Acceptable relative recoveries in the range of 90–106% for fluoride ions were achieved.

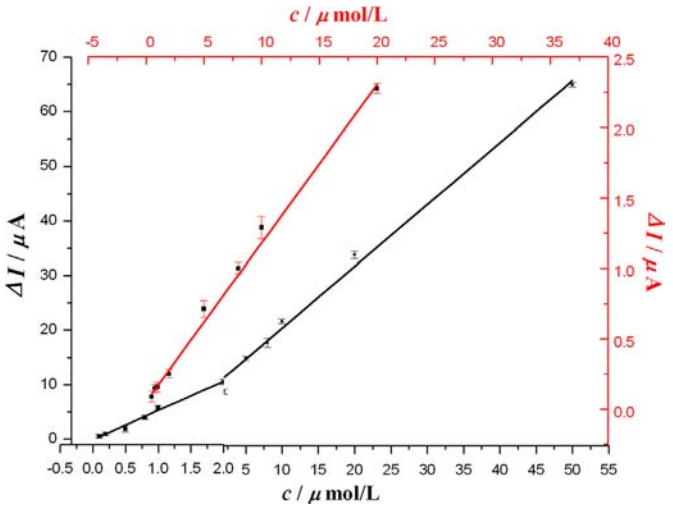

Fig. 7. Calibration curve of fluoride ions at 0.5, 0.8, 1.0, 2.0, 5.0, 8.0, 10.0 and 20.0 μmol/L for the *n*-DCPD/GCE and at 0.1, 0.2, 0.5, 0.8, 1.0, 2.0, 5.0, 8.0, 10.0, 20.0 and 50.0 μmol/L for *n*-HAP/GCE under optimized conditions.

4. Conclusion

In this work, we obtained two porous apatite coatings, dicalcium phosphate dihydrate (DCPD) and hydroxyapatite (HAP) by direct electrodeposition from the electrolyte solution containing $Ca(NO_3)_2 \cdot 4H_2O$ and $NH_4H_2PO_4$. The DCPD and HAP all showed excellent and selective adsorbability to fluoride ions, which can be used as a solid phase microextraction (SPME) fiber and an electrochemical modified electrode. Based on this, a novel indirect strategy for sensitive fluoride ions detection was proposed with voltammetric method using $K_3Fe(CN)_6$ as indicator. The method was applied to extract fluoride ions from three water samples. The results indicated that the indirect method had unique advantages,

Table 1
Determination of fluoride ions in real samples.

Sample[a]	Content found C_x(μmol/L)		Added C_s (μmol/L)		Found after addition $C_{x'}$ (μmol/L)		RSD (%) ($n=3$)		ISE detection $\acute{C}C_0$ (μmol/L) ($n=3$)	Recovery (%)	
	n-DCPD	*n*-HAP	*n*-DCPD	*n*-HAP	*n*-DCPD	*n*-HAP	*n*-DCPD	*n*-HAP		*n*-DCPD	*n*-HAP
Daming lake	5.2	5.6	5.0	5.0	9.8	10.4	7.8	6.7	5.5	92	96
Spouting spring	3.1	3.4	5.0	5.0	7.6	8.0	5.5	4.8	3.2	90	92
Tap water	1.6	1.8	5.0	5.0	6.9	7.0	4.6	5.9	2.0	106	104

[a] The three water samples were diluted for 100 times.

such as easy to perform, rapid to analyze, friendly to human and environment, as well as reliable, simple, fast, sensitive, and cost-effective for fluoride ions detection. Therefore, this method has a great potential of application in the detection of environmental pollutions.

Acknowledgement

This project was supported by the National Basic Research Program of China (No. 2007CB936602).

References

[1] C.L. Arhturhe, J. Pawliszyn, J. Anal. Chem. 62 (1990) 2145–2148.
[2] A. Paschke, P. Popp, J. Chromatogr. A. 1025 (2004) 11–16.
[3] O. Ezquerro, G. Ortiz, B. Pons, M.T. Tena, J. Chromatogr. A. 1035 (2004) 17–22.
[4] M.A. Azenha, P.J. Nogueira, A.F. Silva, J. Anal. Chem. 78 (2006) 2071–2074.
[5] X. Fan, D.J. Parker, M.D. Smith, J. Water Res. 37 (2003) 4929–4937.
[6] M. Mourabet, A. ElRhilassi, H. ElBoujaady, M. Bennani-Ziatni, R. ElHamri, A. Taitai, Appl. Surf. Sci. 258 (2012) 4402–4410.
[7] G. Somer, S. Kalayci, I. Basak, Talanta 80 (2010) 1129–1132.
[8] Z.P. Yang, K. Zhang, F.B. Gong, S.Y. Li, J. Chen, G.Q. Yang, B.A. Trofimov, Beilstein J. Org. Chem. 7 (2011) 46–52.
[9] L. Chen, L. Min, S. Guan, Y.N. Wu, L.J. Xu, F.F. Fu, Food Control. 25 (2012) 433–440.
[10] S. Gao, J. Cui, Z.G. Wei, J. Fluorine Chem 130 (2009) 1035–1041.
[11] M.J. Reyes, M.S. Ríos, J. Hazard. Mater 180 (2010) 297–302.
[12] S. Singh, P. Bhardwaj, V. Singha, S. Aggarwal, U.K. Mandal, J. Colloid Interf. Sci 319 (2008) 322–329.
[13] C. Liang, Z.Y. Li, D.A. Yang, Mater. Chem. Phys. 88 (2004) 285–289.
[14] Y. Song, S.X. Zhang, J.N. Li, C.L. Zhao, X.N. Zhang, Acta Biomater. 6 (2010) 1736–1742.
[15] C.L. He, F. Zhang, L.J. Cao, W. Feng, K.X. Qiu, Y.Z. Zhang, H.S. Wang, X.M. Mo., J.W. Wang, J. Mater. Chem. 22 (2012) 2111–2119.
[16] H. Wang, N. Eliaz, L.W. Hobbs, Mater. Lett. 65 (2011) 2455–2457.
[17] S. Mandel, A.C. Tas, Mater. Sci. Eng., C 30 (2010) 245–254.
[18] L.E.L. Hammari, A. Laghzizil, P. Barboux, K. Lahlil, A. Saoiabi, J. Hazard. Mater. B 114 (2004) 41–44.
[19] Y.W. Fan, Z. Sun, J. Moradian-Oldak, J. Biomater. 30 (2009) 478–483.
[20] C.S. Sundaram, N. Viswanathan, S. Meenakshi, J. Hazard. Mater. 172 (2009) 147–151.
[21] M. Mourabet, A.E. Rhilassi, H.E. Boujaady, M. Bennani-Ziatni, R.E. Hamri, A. Taitai, J. of Saudi Chem. Soc., http://dx.doi.org/10.1016/j.jas.2012.03.003, in press.